Free Radical Biology and Medicine 112 (2017) 376–386

Contents lists available at ScienceDirect

Free Radical Biology and Medicine

journal homepage: www.elsevier.com/locate/freeradbiomed

Original article

Peroxiredoxin-2 plays a pivotal role as multimodal cytoprotector in the early phase of pulmonary hypertension

Enrica Federti[a], Alessandro Matté[a], Alessandra Ghigo[b], Immacolata Andolfo[c], Cimino James[b], Angela Siciliano[a], Christophe Leboeuf[d], Anne Janin[d,e,f], Francesco Manna[c], Soo Young Choi[g], Achille Iolascon[c], Elisabetta Beneduce[a], Davide Melisi[a], Dae Won Kim[g], Sonia Levi[h,i], Lucia De Franceschi[a,*]

[a] Dept. of Medicine, University of Verona-AOUI Verona, Verona, Italy
[b] Molecular Biotechnology Center and Department of Molecular Biotechnology and Health Science, University of Torino, Torino, Italy
[c] CEINGE and Dept. of Biochemistry, University of Naples, Naples, Italy
[d] Inserm, U1165, Paris F-75010, France
[e] Université Paris 7- Denis Diderot, Paris, France
[f] AP-HP, Hôpital Saint-Louis, F-75010 Paris, France
[g] Institute of Bioscience and Biotechnology, Hallym University, Gangwon-do, Republic of Korea
[h] Division of Neuroscience, San Raffaele Scientific Institute, Milano, Italy
[i] Vita-Salute San Raffaele University, Milano, Italy

ARTICLE INFO

Keywords:
Peroxiredoxin-2
Chronic hypoxia
Autophagy
ER stress

ABSTRACT

Pulmonary-artery-hypertension (PAH) is a life-threatening and highly invalidating chronic disorder. Chronic oxidation contributes to lung damage and disease progression. Peroxiredoxin-2 (Prx2) is a typical 2-cysteine (Cys) peroxiredoxin but its role on lung homeostasis is yet to be fully defined. Here, we showed that $Prx2^{-/-}$ mice displayed chronic lung inflammatory disease associated with (i) abnormal pulmonary vascular dysfunction; and (ii) increased markers of extracellular-matrix remodeling. Hypoxia was used to induce PAH. We focused on the early phase PAH to dissect the role of Prx2 in generation of PAH. Hypoxic $Prx2^{-/-}$mice showed (i) amplified inflammatory response combined with cytokine storm; (ii) vascular activation and dysfunction; (iii) increased PDGF-B lung levels, as marker of extracellular-matrix deposition and remodeling; and (iv) ER stress with activation of UPR system and autophagy. Rescue experiments with *in vivo* the administration of fused-recombinant-PEP-Prx2 show a reduction in pulmonary inflammatory vasculopathy and in ER stress with down-regulation of autophagy. Thus, we propose Prx2 plays a pivotal role in the early stage of PAH as multimodal cytoprotector, targeting oxidation, inflammatory vasculopathy and ER stress with inhibition of autophagy. Collectively, our data indicate that Prx2 is able to interrupt the hypoxia induced vicious cycle involving oxidation-inflammation-autophagy in the pathogenesis of PAH.

1. Introduction

Pulmonary artery hypertension (PAH) is a life threatening highly invalidating chronic disorder [1–3]. Although in the last decade progresses have been made in the identifications of factors involved in its pathogenesis, much still remains to be investigated in the mechanism involved in the early stage of PAH [3–5]. Regardless of the initial event, the combination of chronic inflammation and chronic

Abbreviations: PAH, pulmonary artery hypertension; PBS, phosphate buffer; qRT-PCR, quantitative real time; ARDS, acute respiratory distress syndrome; ARE, anti-oxidant responsive element; Atg4, autophagy related 4; ATF6, activating transcription factor 6; Chop, C/EBP [CCAAT/enhancer-binding protein]-homologous protein; BAL, bronchoalveolar lavage; ET-1, endothelin 1; ER, endoplasmic reticulum; GAPDH, glyceraldehyde 3-phosphate dehydrogenase; HO-1, heme oxygenase 1; HSP, heat shock protein; HY stress, hypoxia stress; IRE1, inositol-requiring 1; IL-1b, interleukin 1b; IL-6, interleukin 6; IL-10, interleukin 10; LPS, lipopolysaccharides; NAC, N-acetyl-cysteine; NF-kB, nuclear factor kappa-light-chain-enhancer of activated B cells; Nrf2, nuclear factor-erythroid 2; PAH, pulmonary artery hypertension; PDGF-B, Platelet-derived growth factor subunit B; PEP Prx2, Prx2 fused to cell penetrating carrier PEP1 peptide; Prx2, peroxiredoxin-2; SMCs, smooth muscle cells; SOD-1, superoxide dismutase 1; Trdx, Thioredoxin reductase; PERK, PKR-like endoplasmic reticulum kinase; UPR, unfolded protein response; sXbp1, spliced X-box binding protein 1; GADD34, growth arrest and DNA damage-inducible protein; VCAM-1, vascular cell adhesion molecule 1; MDA, malondialdehyde; RV, right ventricular; RVSP, right ventricular systolic pressure; PAT, pulmonary acceleration time; ET, ejection time; ICAM-1, intercellular adhesion molecule 1; ANP, atrial natriuretic peptide; Ulk 1, Serine/threonine-protein kinase Ulk1; LC3 I/II, microtubule-associated protein 1A/1B-light chain 3

* Correspondence to: Dept of Medicine, University of Verona- AOUI Verona, Policlinico GB Rossi- P.le L Scuro, 10, 37134 Verona, Italy.
E-mail address: lucia.defranceschi@univr.it (L. De Franceschi).

http://dx.doi.org/10.1016/j.freeradbiomed.2017.08.004
Received 9 May 2017; Received in revised form 2 August 2017; Accepted 4 August 2017
Available online 09 August 2017

hypoxia promote a high pro-oxidant environment, mediating disease progression [1,2,4,6,7].

In this scenario, efficient catabolic pathways to either buildup misfolded/unfolded proteins or to clear intracellular damaged proteins are required [8–11]. Studies in different models of PAH have shown that cellular response to face the accumulation of damaged proteins is mainly through endoplasmic reticulum (ER) stress followed by the activation of autophagy to clear damaged proteins and to reduce ER stress [10,12,13]. Indeed, classic chaperones such as heat shock protein 90 and 70 (HSP) are upregulated in PAH, indicating the requirement of chaperone systems to deal with the accumulation of damaged proteins [14].

Prx2 is a typical 2-cysteine (Cys) peroxiredoxin ubiquitously expressed. Prx2 has been largely investigated in erythroid cells, where it is able to scavenge low concentration of H_2O_2 without inactivation due to over-oxidation [15]. Recently, in different cell models, Prx2 has been also linked to chaperone activity, priming cells to better tolerate oxidation [16,17]. Studies in mouse genetically lacking Prx2 ($Prx2^{-/-}$) have highlighted its protective role against LPS induced lethal shock and acute distress syndrome (ARDS), suggesting a possible contribution of Prx2 in inflammatory response [17–23]. In addition, *in vitro* and *in vivo* model of ischemic/reperfusion stress highlighted the key role of Prx2 as anti-oxidant system [24,25].

Here, we studied the role of Prx2 in development of pulmonary hypertension in mice genetically lacking Prx2 ($Prx2^{-/-}$), using hypoxic stress to explore the early stage of early phase of pulmonary hypertension. Our data collectively indicate that Prx2 plays a pivotal role in the early phase of hypoxia induced pulmonary hypertension as anti-oxidant system and chaperone. The administration of Prx2 fused to cell-penetrating carrier PEP (cell penetrating peptide; PEP Prx2; [19]) (i) reduces local and systemic inflammation; (ii) prevents vascular activation and PDGF-B up-regulation; (iii) alleviates ER stress and (i) down-regulates autophagy activation in response to hypoxia. Thus, PEP Prx2 might represent an interesting new multimodal therapeutic option in the early stage PAH.

2. Materials and methods

2.1. Drugs and chemicals

Details are reported in Supplemental materials and methods.

2.2. Mouse strains and design of the study

C57B6/2J mice as wildtype controls (WT) and $Prx2^{-/-}$ mice aged between 4 and 6 months both male and female were used in the present study [19,26]. The Institutional Animal Experimental Committee, University of Verona (CIRSAL) and by the Italian Ministry of Health approved the experimental protocols. Where indicated WT and $Prx2^{-/-}$ mice were treated with 1) N-Acetyl-Cysteine (NAC) at the dosage of 100 mg/kg/d (in NaCl 0.9%, NaOH 36 mM, pH 9.4; ip) or vehicle only for 3 weeks [19,20]; 2) PEP Prx2 (in PBS) or vehicle at the dosage of 3 mg/kg/d ip or vehicle for 4 weeks before and during hypoxia [19]. Whenever indicated, mice were exposed to hypoxia (8% oxygen for 10 h, 3 days, 7 days) (Hy) as previously described [27–29]. To collect organs, animals were first anesthetized with isoflurane, bronchoalveolar lavage (BAL) was collected and then mice were euthanized. Organs were immediately removed and divided into two and either immediately frozen in liquid nitrogen or fixed in 10% formalin and embedded in paraffin for histology.

2.2.1. Bronchoalveolar lavage (BAL) measurements

BAL fluids were collected and cellular contents were recovered by centrifugation and counted by microcytometry as previously reported [27]. Percentage of neutrophils was determined on cytospin centrifugation. Remaining BAL samples were centrifuged at 1500 × *g* for 10 min at 4 °C. The supernatant fluids were used for determination of total protein content [27].

2.3. Lung molecular analysis

2.3.1. Lung histology

Multiple (at least five) three-micron whole mount sections were obtained for each paraffin-embedded lung and stained with hematoxylin eosin, Masson's trichome, and May-Grünwald-Giemsa. α-smooth muscle actin immunohistochemistry (IHC) on lungs was carried out as previously reported [27,30]. Lung pathological analysis was carried out by blinded pathologists as previously described [27,30]. Based on previous reports (18, 38), the pathological criteria for lung histopathology were as follows: i) Bronchus: Mucus: 0: no mucus; +: mucus filling less than 50% of the area of the bronchus section; ++: mucus filling more than 50% of the area of the bronchus section. (ii) Inflammatory infiltrate density: 0: less than 5 inflammatory cells per field; +: 5–30 inflammatory cells per field; ++ more than 30 inflammatory cells per field. (iii) Thrombi: 0: no thrombus; + presence of a thrombus in one field, at magnification 250.

2.3.2. Immunoblot analysis

Frozen lung and heart from each studied group were homogenized and lysed with iced lyses buffer (LB containing: 150 mM NaCl, 25 mM bicine, 0.1% SDS, Triton 2%, EDTA 1 mM, protease inhibitor cocktail tablets (Roche), 1 mM Na_3VO_4 final concentration) then centrifuged 10 min at 4 °C at 12,000*g*. Proteins were quantified and analyzed by mono-dimensional SDS polyacrylamide gel electrophoresis. Gels were transferred to nitrocellulose membranes for immuno-blot analysis with specific antibody. Details are reported in Supplemental materials and methods [21,27,31–33]. Whenever indicated Prx2 dimerization was studied in lung from PBS perfused mice containing 100 mM NEM, using an approach similar to that reported by Kumar et al. [34].

2.3.3. RNA isolation, cDNA preparation and quantitative RT-PCR

Total RNA was extracted from tissues using Trizol reagent (Life Technologies, Monza, Italy). Synthesis of cDNA from total RNA (1 μg) was performed using Super Script II First Strand kits (Life Technologies). Quantitative RT-PCR (qRT- PCR) was performed using the SYBR-green method, following standard protocols with an Applied Biosystems ABI PRISM 7900HT Sequence Detection system. Relative gene expression was calculated using the $2^{(-\Delta Ct)}$ method, where ΔCt indicates the differences in the mean Ct between selected genes and the internal control (GAPDH). qRT-PCR primers for each gene were designed with Primer Express 2.0 (Life Technologies) (primer sequences are reported in Table 1S) [27,30].

2.4. MDA assay

MDA was determined as previously reported [35].

2.5. Evaluation of right ventricular hypertrophy and echocardiography measurements

Hearts were fixed with 10% formaldehyde for 24 h. The right ventricular (RV) free wall was separated from the left ventricular with septum (LV + S) under dissection microscope. RV and LV + S were separately weighed and used to calculate the ratios RV/(LV + S)/body weight [36]. Transthoracic echocardiography was performed with a Vevo 2100 echocardiograph (Visual Sonics, Toronto, Canada) equipped with a 22–55 MHz transducer (MicroScan Transducers, MS500D) as previously reported [27,37].

2.6. Statistical analysis

Data were analyzed using either *t*-test or the 2-way analysis of

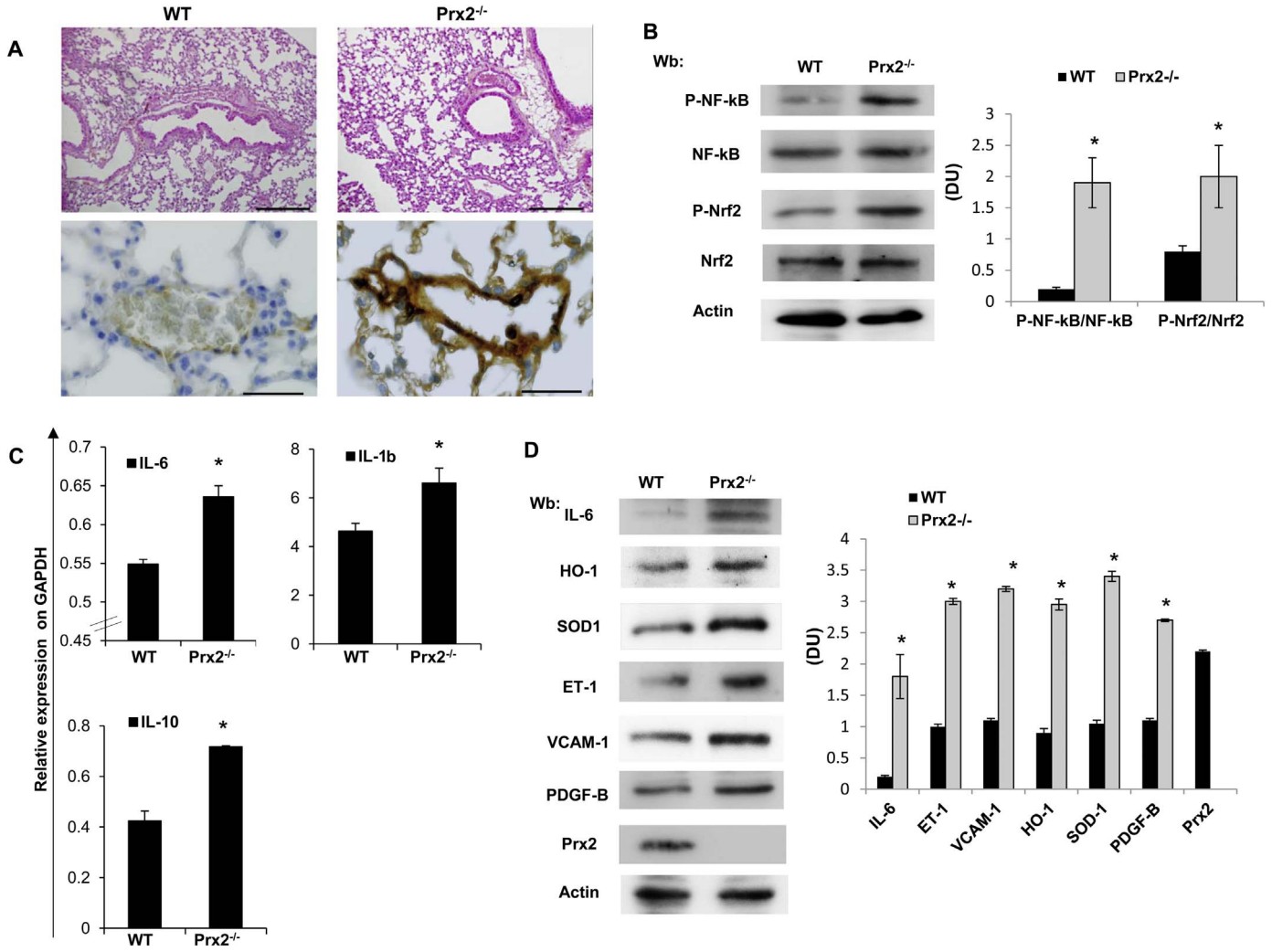

Fig. 1. The absence of Prx2 promotes lung inflammation, increased pulmonary vascular activation and extra-matrix remodeling markers. A. Comparison of Prx2$^{-/-}$ with WT mice shows an increased peribronchial edema in Prx2$^{-/-}$ mice (upper panel Hematoxylin Eosin ×250) and deposits of alpha actin in vascular walls in Prx2$^{-/-}$ mice (lower panel Immunohistochemistry using anti alpha actin antibody × 600). **B**. Immunoblot analysis with specific antibodies against phospho-NF-kB (P-NF-kB), NF-kB, phospho-Nrf2 (P-Nrf2) and Nrf2 of lung from wildtype (WT) and Prx2$^{-/-}$ mice under normoxic condition. One representative gel from six with similar results is presented. **Right panel**. Densitometric analysis (DU: Density Units) of immunoblots is shown as means ± SD (n = 6); *p < 0.05 compared to wildtype. **C**. IL-6, IL-1b, IL-10 mRNA levels in lung tissues (normalized to GADPH) from WT and Prx2$^{-/-}$ mice. * p < 0.05 (WT vs Prx2$^{-/-}$). Each sample (WT; Prx2$^{-/-}$) is a pool from 5 mice. Representative of three independent experiments. **D**. Immunoblot analysis with specific antibodies against IL-6, heme-oxygenase 1 (HO-1), endothelin-1 (ET-1), superoxide dismutase (SOD-1), vascular cell adhesion molecule-1 (VCAM-1), platelet derived growth factor-B (PDGF-B) and peroxiredoxin-2 (Prx2) of lung from wildtype (WT) and Prx2$^{-/-}$ mice under normoxic condition. One representative gel from six with similar results is presented. **Right panel**. Relative quantification of immunoreactivity (DU: Density Units) of IL-6, HO-1, SOD1, ET-1, VCAM1, PDGF-B and Prx2 of lung from wildtype (WT) and Prx2$^{-/-}$ mice under normoxic condition. Data are shown as means ± SD (n = 6); *p < 0.05 compared to wildtype.

variance (ANOVA) for repeated measures between the mice of various genotypes. A difference with a P value less than 0.05 was considered significant.

3. Results

3.1. Mice genetically lacking Prx2 show lung inflammation, increased pulmonary vascular activation and extracellular-matrix remodeling

Lung histopathologic analysis showed increased peribronchial edema without changes in the number of mucus cells in Prx2$^{-/-}$ mice under normoxia compared to wildtype animals (Fig. 1A, upper panel). The systematic study for α-smooth cells expression showed a staining in broken line only on bronchial sections of Prx2$^{-/-}$ mice, suggesting an initial pulmonary vessel muscularization (Fig. 1A, lower panel). Increased bronchoalveolar lavage (BAL) levels of proteins and of total leukocytes were detected in Prx2$^{-/-}$ mice compared to wildtype, indicating an abnormal pulmonary vascular leakage (Fig. 1SA).

In Prx2$^{-/-}$ mice, we observed increased active form of NF-kB and Nrf2, two redox related transcriptional factors, compared to wildtype animal (Fig. 1B).

This was associated with increased lung MDA levels (Fig. 1SB) and up-regulation of the pro-inflammatory cytokines IL-6, IL-1b and IL10 that are known targets of NF-kB (Fig. 1C). We confirmed the increased expression of IL-6 by immunoblot analysis in lung from Prx2$^{-/-}$ mice compared to wildtype animals (Fig. 1D). The activation of Nrf2 in the absence of Prx2 was supported by the up-regulation of Nrf2 related systems such as HO-1, a vascular and lung cytoprotector, and SOD-1, a potent anti-oxidant enzyme supports (Fig. 1D) [38]. We also observed higher levels of (i) endothelin-1 (ET-1), the most potent vasoconstrictive and broncho-constrictive cytokine [30]; (ii) VCAM-1, a marker of vascular endothelial activation [27]; and (iii) PDGF-B, a known factor involved in lung extra-cellular matrix remodeling [39] (Fig. 1D).

These data link the absence of Prx2 with persistent lung inflammation, endothelial vascular activation, and extracellular matrix remodeling.

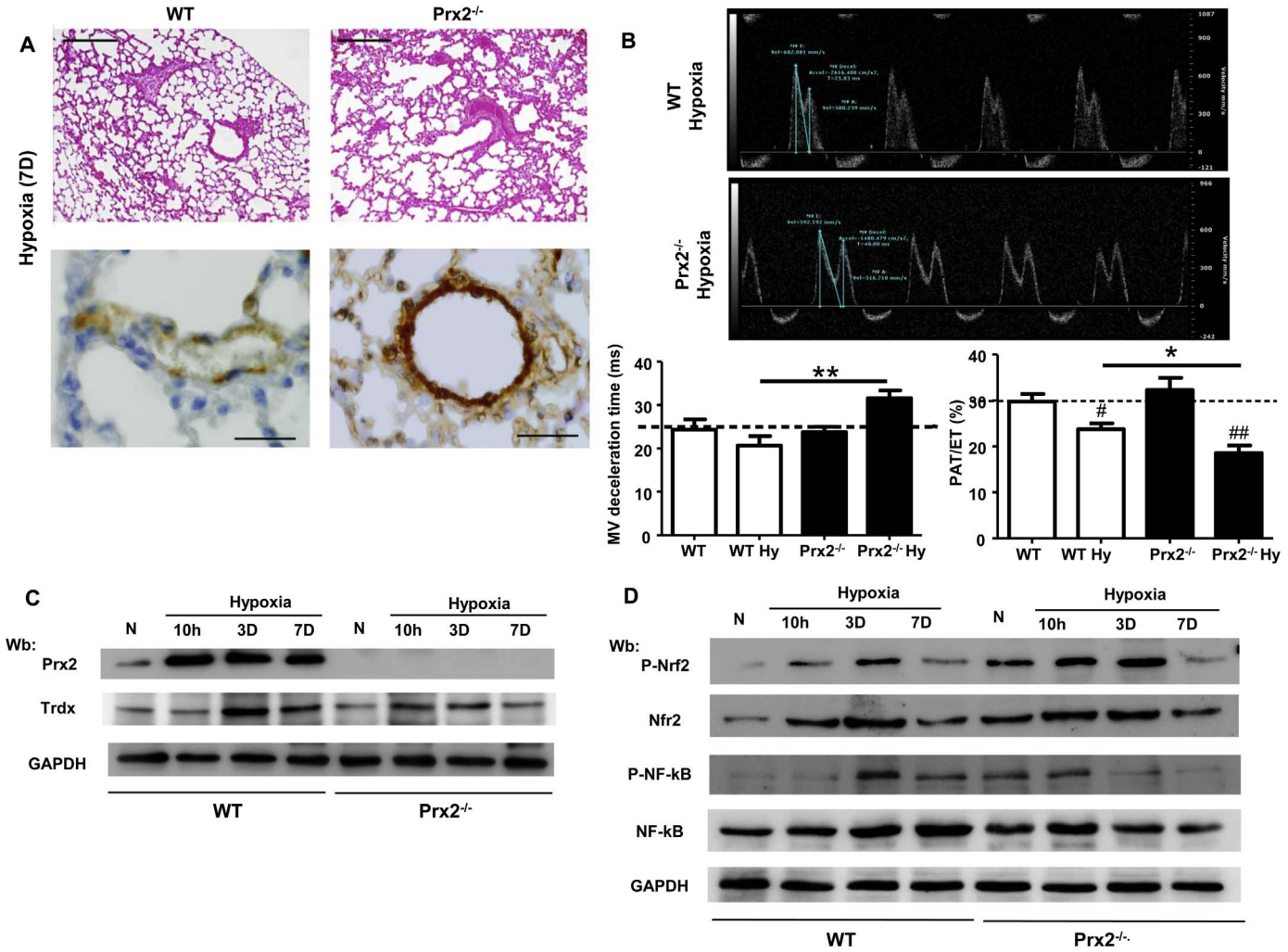

Fig. 2. In Prx2$^{-/-}$ mice, hypoxia induces early stage pulmonary hypertension and is associated with activation of redox-related transcriptional factors. A. Comparison of Prx2$^{-/-}$ with WT mice shows a sparse inflammatory infiltrate and an increased peribronchial edema in Prx2$^{-/-}$ mice (upper panel Hematoxylin Eosin ×250) and deposits of alpha actin in vascular walls in Prx2$^{-/-}$ mice (lower panel Immunohistochemistry using anti alpha actin antibody × 600). **B.** Representative images of mitral inflow pattern recorded by Doppler echo imaging in wildtype (WT) and Prx2$^{-/-}$ mice under hypoxia as in Fig. 1A. **Lower panels**. Average mitral valve deceleration time (left panel) and pulmonary acceleration time (PAT) to ejection time (ET) ratio (right panel). *p < 0.05 and **p < 0.01 WT *vs* Prx2$^{-/-}$ mice; #p < 0.05 and ##p < 0.01 hypoxia *vs* basal by one-way ANOVA followed by Newman-Keuls Multiple Comparison test. The black dashed lines have been added to the graph to favor visual comparison between the white bars *vs* the black bars. **C.** Immunoblot analysis with specific antibodies against peroxiredoxin-2 (Prx2) and thioredoxin-reductase 1 (Trdx) of lung wildtype (WT) and Prx2$^{-/-}$ mice under normoxia (N) exposed to hypoxia) for 10 h (10 h), 3 days (3D), 7 days (7D). One representative gel from six with similar results is presented. Densitometric analysis of immunoblots is shown in Fig. 2SA. **D.** Immunoblot analysis with specific antibodies against phospho-NF-kB (P-NF-kB), NF-kB, phospho-Nrf2 (P-Nrf2) and Nrf2 of lung wildtype (WT) and Prx2$^{-/-}$ mice under normoxia (N) and exposed to hypoxia (Hy) for 10 h (10 h), 3 days (3D), 7 days (7D). One representative gel from six with similar results is presented. Densitometric analysis of immunoblots is shown in Fig. 2SB.

3.2. Prolonged hypoxia promotes the development of early stage pulmonary hypertension in Prx2$^{-/-}$ mice

Based on our previous report, showing the development of early stage PAH in a mouse model for sickle cell disease but not in wildtype mice [36], we exposed both mouse strains to hypoxia (Hy) 8% oxygen for 7 days. As shown in Fig. 2A, hypoxia induced sparse inflammatory cell infiltrate with some peribronchial edema in Prx2$^{-/-}$ mice. On the bronchial epithelium there was no significant change in the number of mucus cells in both mouse strains. On vascular sections, no thrombus was found in any of the mouse groups. The systematic study for α-actin deposition revealed the presence of almost linear staining around bronchial and vascular sections in Prx2$^{-/-}$ mice (Fig. 2A, lower panel). While, α-actin depositions were sparse in hypoxic wildtype mice.

We evaluated the presence of RV hypertrophy in both mouse strains exposed to 7days hypoxia. In Prx2$^{-/-}$ mice, we observed a slight but significant increase in RV/(LV + S) ratio (normoxia: 0.21 ± 0.03 *vs* hypoxia 0.34 ± 0.05; $n = 6$, $P < 0.05$), whereas no changes were observed in wildtype mice in agreement with our previous report [36]. This was associated with a significant increase in mitral valve deceleration time and a reduction in pulmonary acceleration time/ ejection time ratio (Fig. 2B), indicating early diastolic dysfunction and increased right ventricular systolic pressure in Prx2$^{-/-}$ mice. In addition, we found hypoxia induced increased expression of SOD-1 in heart from both mouse strains, but to a higher extent in Prx2$^{-/-}$ mice (Fig. 1SD). Hypoxia induced up-regulation of (i) VCAM-1 and ICAM-1; and (ii) atrial natriuretic peptide (ANP) was also observed in both mouse strains (Fig. 1SD).

Our findings are consistent with the development of early stage of PAH promoted by severe oxidation and amplified inflammatory response in Prx2$^{-/-}$ mice exposed to 7-days hypoxia.

3.3. Prx2 plays an important role as cytoprotective system against hypoxia induced PAH

In order to follow-up the generation of PAH in Prx2$^{-/-}$ mice, we studied both mouse strains at different time intervals between 0 to 7-days hypoxia to identify the optimal window-time to analyze

mechanism(s) involved in development of PAH. BAL protein and leukocyte count were significantly increased in Prx2$^{-/-}$ mice during hypoxia at 10 h, 3 days and 7 days compared to wildtype animals (data not shown).

Hypoxia markedly increased Prx2 expression in lung from wildtype mice at 10 h, 3 days and 7 days of exposure (Fig. 2C; Fig. 2SA). This was associated with time dependent increased expression of thioredoxin-reductase, a Prx2 repairing system (Trdx; Fig. 2C; Fig. 2SA). The modulation of Trdx expression during hypoxia even in the absence of Prx2, may be possible related to the fact that Trdx is part of different NADPH-dependent pathways [19,40].

In Prx2$^{-/-}$ mice exposed to hypoxia, we observed a rapid and sustained activation of Nrf2 in response to hypoxia, while there was a reduction in activation of NF-kB (Fig. 2D, 2SB). Otherwise, wildtype mice showed an early response of Nrf2 at 10 and 3-h hypoxia, partially overlapping the activation of NF-kB observed at 3 and 7 days hypoxia (Figs. 2D, 2SB). These data suggest that Nrf2 might be a precocious back-up mechanism in response to hypoxia, which is early activated in both mouse strains, but to higher extent in mice genetically lacking Prx2.

Since pro-inflammatory cytokines are modulated by oxidation and participates to the development of PAH [3,41,42], we evaluated IL1b and IL6 expression in lung from both mouse strains during hypoxia. In Prx2$^{-/-}$ mice, IL-1b mRNA levels were significantly increased at 3 days of hypoxia compared to wildtype animals, which displayed increased IL-1b expression only at 7-days hypoxia (Fig. 3A). In Prx2$^{-/-}$ mice, lung IL-6 mRNA expression was significantly upregulated at 3 days of hypoxia followed by a decreased at 7 days of hypoxia to levels still higher than those observed in wildtype mice (Fig. 3B). These data support an earlier and amplified inflammatory response in Prx2$^{-/-}$ mice in response to hypoxia compared to wildtype animals.

We then evaluated markers of pulmonary vascular remodeling (ET-1, PDGF-B, ANP) and vascular endothelial activation (VCAM-1 and ICAM-1). As shown in Fig. 3C, ET-1 expression was increased in both mouse strains but to a higher extent in Prx2$^{-/-}$ mice compared to wildtype; while PDGF-B levels increased earlier, reaching higher and constant levels in Prx2$^{-/-}$ mice compared to wildtype during hypoxia. VCAM-1 and ICAM-1 expression was similarly increased in both mouse strains at 7 days hypoxia (Fig. 3D). Whereas, ANP levels were higher in Prx2$^{-/-}$ mice than in wildtype animals exposed to prolonged hypoxia (Fig. 3D).

Collectively, these data indicate that the absence of Prx2 accelerates vascular activation and extra-cellular matrix remodeling, amplifying inflammatory response and oxidation during hypoxia.

3.4. The absence of Prx2 is associated with endoplasmic reticulum (ER) stress and up-regulation of ATF6

Studies in different models of PAH have shown that hypoxia and/or PDGF-B and /or ET-1 induce severe proteins damage, which promotes endoplasmic reticulum stress (ER), triggering unfolded protein response (UPR) system [10,11,13,43]. When the accumulation of damaged proteins exceeds the ER capacity, ER stress leads to activation of autophagy as adaptive mechanism to clear accumulated misfolded/unfolded proteins [11,44]. UPR system is characterized by 3 branches: IRE, PERK and ATF6, this latter has been reported to be mainly involved in PAH [12,45]. As shown in Fig. 4A, ATF6, Chop and sXbp1 were up-regulated in lung from Prx2$^{-/-}$ mice under normoxia compared to wildtype animals. Whereas, GADD34 was downregulated in Prx2$^{-/-}$ mice compared to wildtype animals (Fig. 4A). In response to hypoxia, we observed dynamic changes of the main UPR systems: (i) ATF6; (ii) GADD34 and Chop, related to PERK and Xbp1, a component of IRE branch [10]. As shown in Fig. 4B, increased mRNA levels of both Chop and Xbp1 were observed at 10 h in Prx2$^{-/-}$ mice, while GADD34 was still significantly increased at 3-days hypoxia compared to normoxic Prx2$^{-/-}$ animals. In chronically exposed Prx2$^{-/-}$ mice, ATF6 and sXbp1 mRNA levels were again higher than in normoxia Prx2$^{-/-}$ animals (Fig. 4B). Wildtype animals show an early signs of ER stress with up-regulation of ATF6 and Xbp1 at 10-h hypoxia, with no major change in chronic hypoxia (Fig. 4B). It is of note that in lung from wildtype mice, we found Prx2 organized in multimers, possible reflecting the acquisition of chaperone like function (data not shown) [31,46,47].

These data indicate that the absence of Prx2 triggers ER stress during hypoxia, contributing to the early appearance of PAH in Prx2$^{-/-}$ mice.

3.5. PEP Prx2 treatment rescues prolonged hypoxia induced heart and lung inflammatory vasculopathy and prevents ER stress

To address the question whether Prx2 plays a role in lung chronic inflammatory disease, we firstly evaluated the impact of recombinant fusion protein PEP Prx2 (1.5 mg/kg/day ip; 3 weeks) to both mouse strains under room air condition. In normoxic Prx2$^{-/-}$ mice, PEP Prx2 treatment (i) prevented Nrf2 and NF-kB activation (Fig. 3SA); (ii) reduced HO-1 protein expression (Fig. 3SB); and (iii) decreased the levels of ET-1, VCAM-1 and PDGF-B (Fig. 3SB). No major changes were observed in wildtype animals (Fig. 3SA, 3SB). In order to evaluate whether the effects of PEP Prx2 treatment were specific of Prx2 or related to a general anti-oxidant effect, we treated both mouse strains with NAC (100 mg/kg/day for 3 weeks), a known anti-oxidant agent previously used in other *in vitro* and *in vivo* models of PAH [6,48]. No changes were present in the levels of Nfr2 and NF-kB activation in Prx2$^{-/-}$ mice treated with NAC, suggesting that the effects of PEP Prx2 are peculiar of Prx2 and not only related to its general antioxidant effects (data not shown).

In Prx2$^{-/-}$ mice exposed to 7 days hypoxia, PEP Prx2 treatment significantly reduced the hypoxia mediated diastolic dysfunction and ameliorated RVSP, as suggested by the increased in PAT/ET ratio (Fig. 4C, 4SA). In agreement, in heart from PEP Prx2 treated Prx2$^{-/-}$ mice exposed to 7 days hypoxia, we found a reduction of ANP expression as well as of markers of vascular endothelial activation (Fig. 4D). This was associated with a decrease in levels of SOD-1 and in oxidation of proteins from heart of hypoxic Prx2$^{-/-}$ mice treated with PEP Prx2 (Fig. 4SB). We found similar evidences of the beneficial effects of PEP Prx2 on lung from Prx2$^{-/-}$ mice exposed to prolonged hypoxia. As shown in Fig. 5A, PEP Prx2 promoted a significant reduction in chronic hypoxia induced increase of ANP, VCAM-1, ICAM-1 and PDGF-B levels compared to vehicle treated Prx2$^{-/-}$ animals. In addition, PEP Prx2 decreased the hypoxia induced ATF6 expression, suggesting a possible role of Prx2 as chaperone in agreement with the reduced expression of classic chaperone HSP70 and 90 (Fig. 5B).

To better understand the role of Prx2 in development of PAH, we chose to further study Prx2$^{-/-}$ mice at day 3 of hypoxia. This represents the turning point in the imbalance between oxidation/anti-oxidant activities and the activation of cellular defense mechanisms against cytotoxic effects of accumulation of damage proteins. Indeed, we found a significant increase in the amount of Prx2 dimers in lung from wildtype after 3 days hypoxia compared to normoxic wildtype animals (Fig. 4SC), supporting the role of Prx2 as H_2O_2 sensor generated during hypoxia as previously shown in other models [34,49].

3.6. In Prx2$^{-/-}$ mice, PEP Prx2 prevents the hypoxia induced oxidative stress and reduces inflammatory vascular activation and extracellular matrix remodeling

PEP Prx2 administration prevented the hypoxia induced increased in BAL protein and leukocyte content in both mouse strains (Fig. 4SD). This was associated with a marked reduction in protein oxidation state in both mouse strains exposed to 3 days hypoxia and treated with PEP Prx2, supporting the local anti-oxidant effect of exogenous PEP Prx2 treatment during hypoxia stress (Fig. 5C). In agreement, we found that PEP Prx2 administration prevented the hypoxia induced Nrf2 and NF-kB activation in both mouse strains (Fig. 5D, 5SA). This was paralleled

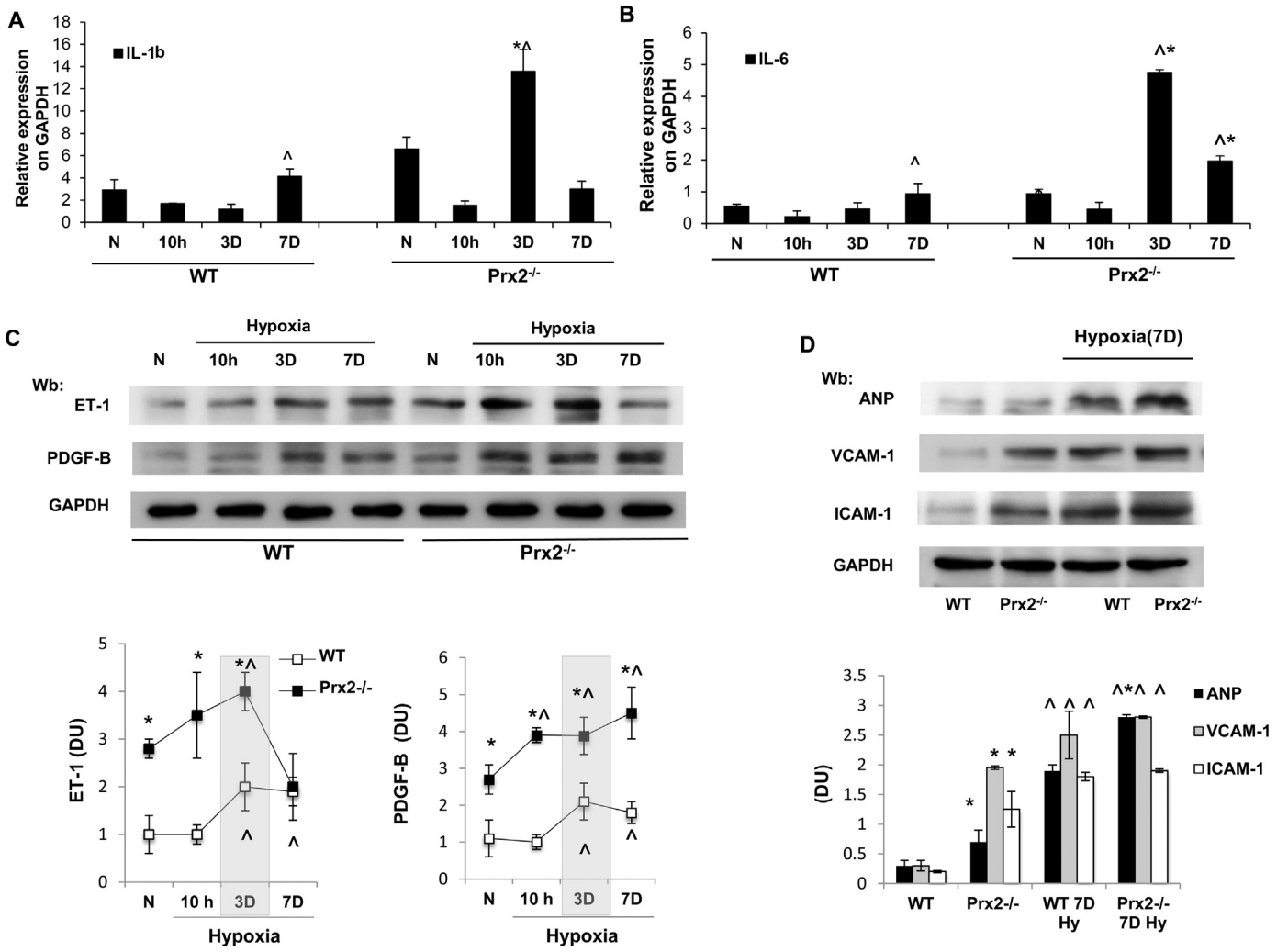

Fig. 3. In Prx2$^{-/-}$ mice, hypoxia is associated with amplified inflammatory response, vascular activation and increased expression of PDGF-B, a marker of extracellular matrix remodeling. A-B. IL-1b (**A**) and IL-6 (**B**) mRNA levels in lung tissues (normalized to GADPH) wildtype (WT) and Prx2$^{-/-}$ mice under normoxia (N) and exposed to hypoxia for 10 h (10 h), 3 days (3D), 7 days (7D). *p < 0.05 compared to wildtype; ^ p value < 0.05 compared to normoxic mice. Each sample is a pool from 5 mice. Representative of three independent experiments. **C. Upper panel**. Immunoblot analysis with specific antibodies against endothelin-1 (ET-1) and platelet derived growth factor-B (PDGF-B) of lung from wildtype (WT) and Prx2$^{-/-}$ mice under normoxia (N) and exposed to hypoxia for 10 h (10 h), 3 days (3D), 7 days (7D). One representative gel from six with similar results is presented. **Lower panel**. Relative quantification of immunoreactivity (DU: Density Units) of ET-1 and PDGF-B in lung from wildtype (WT) and Prx2$^{-/-}$ mice under normoxia (N) and exposed to hypoxia for 10 h (10 h), 3 days (3D), 7 days (7D). Data are shown as means ± SD (n = 6). *p < 0.05 compared to wildtype; ^ p < 0.05 compared to normoxic mice. The grey area highlights the changes in the ET-1 and PDGF-B expression in the mouse strains at 3 days hypoxia. **D. Upper panel**. Immunoblot analysis with specific antibodies against atrial natriuretic peptide (ANP), vascular adhesion molecule -1 (VCAM-1) and intracellular adhesion-molecule- 1 (ICAM-1) of lung from wildtype (WT) and Prx2$^{-/-}$ mice under normoxia (lane 1 and 2) and exposed to 7 days (7D) hypoxia. One representative gel from six with similar results is presented. **Lower panel**. Relative quantification (DU: Density Units) of immunoreactivity of ANP, VCAM-1, ICAM-1 in lung from wildtype (WT) and Prx2$^{-/-}$ mice under normoxia and exposed to 7 days (7D) hypoxia. Data are shown as means ± SD (n = 6); *p < 0.05 compared to wildtype; ^ p < 0.05 compared to normoxic mice.

by the reduction in HO-1, IL-6, ET-1, VCAM-1 and PDGF-B (Fig. 6A).

These data suggest that PEP Prx2 treatment during hypoxia is able to (i) decrease local pulmonary inflammation and oxidation, (ii) reduce systemic inflammatory response; (iii) beneficially affect hypoxia abnormalities in pulmonary vascular leakage; and (iv) prevent hypoxia activation of redox-sensitive transcriptional factors Nrf2 and NF-kB.

3.7. PEP Prx2 alleviates ER stress and down-regulates autophagy in Prx2$^{-/-}$ mice exposed to hypoxia

As shown in Fig. 6B, PEP Prx2 significantly down-regulated G-ADD34 in lung from Prx2$^{-/-}$ mice compared to vehicle treated animals. This was associated with a marked decrease in HSP70 and 90 expression in lung from both mouse strains exposed to 3 days hypoxia and treated with PEP Prx2 (Fig. 6C). This is agreement with previous reports on preventing PAH development by blocking ER stress with exogenous chemical chaperones [12].

Since a link between ER stress and activation of autophagy has been proposed to deal the accumulation of damaged proteins [10,44], we evaluated key elements of autophagy machinery and the effects of PEP Prx2 treatment in both mouse strains at 3 days hypoxia. Based on revision of the literature, we chose to analyze the expression of (i) autophagy related proteins ULk1 that is required for initiation of autophagy; (ii) LC3 I/II, a coordinator of phagosomal membranes and (iii) p62, a key cargo protein and component of inclusion bodies; and (iv) pro-caspase 3/caspase 3, involved in digestion of damaged proteins [9,50–52]. As shown in Fig. 7A, normoxic Prx2$^{-/-}$ mice showed increased LC3-II formation associated with increased expression of Ulk1 and p62 compared to wildtype mice. This was associated with higher expression of pro-caspase 3/caspase 3, indicating an activation of autophagy to clear intracellular oxidative damaged proteins in Prx2$^{-/-}$ mice. In both mouse strains, hypoxia markedly activated autophagy as supported by increased LC3I/II expression, consumption of Ulk1 and reduction of p62, suggesting a clearance of p62 positive inclusion

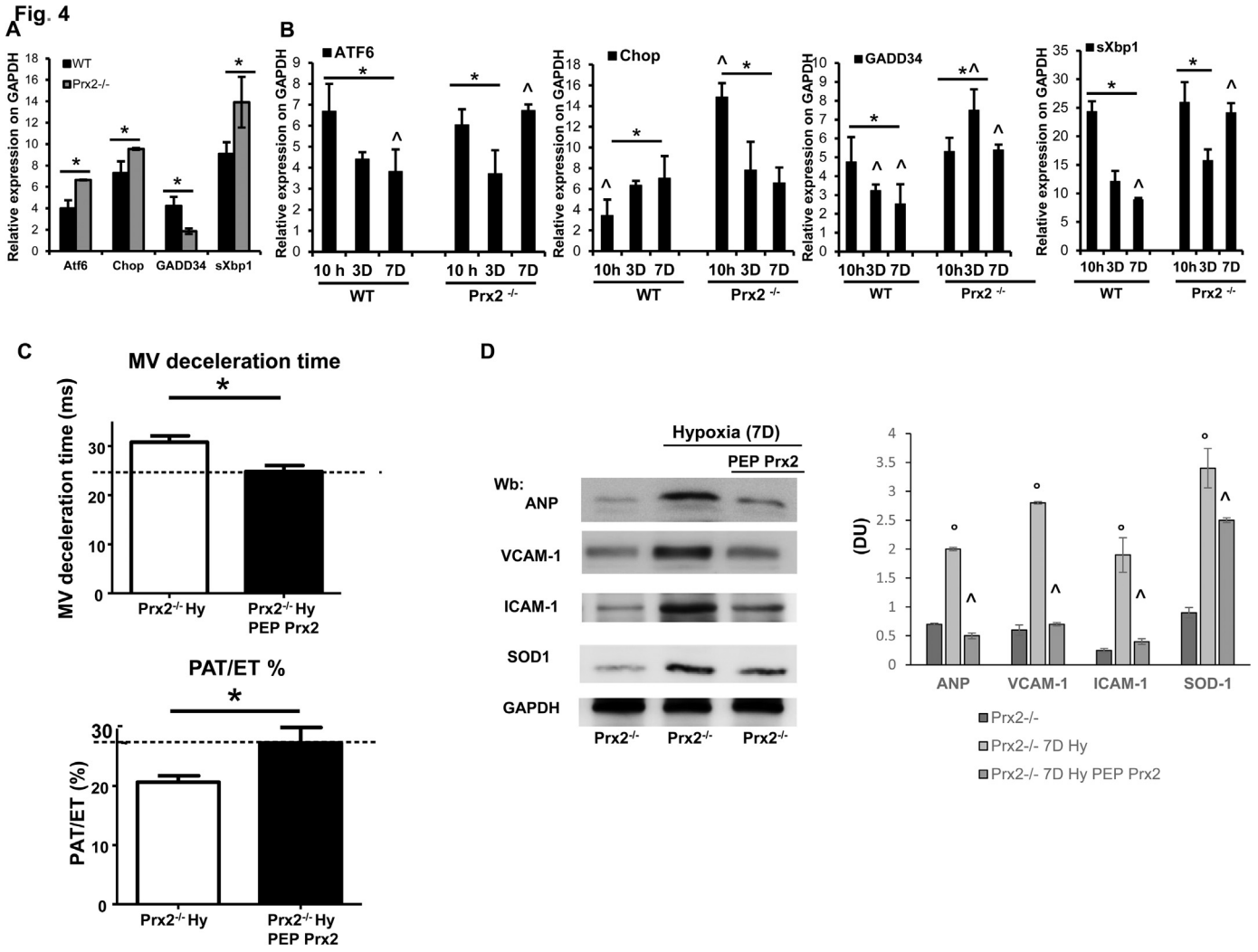

Fig. 4. Hypoxia induces ER stress in Prx2$^{-/-}$ mice and PEP Prx2 administration prevents the hypoxia induced diastolic dysfunction with reduction of inflammatory vasculopathy. A-B. ATF6, CHOP, GADD34, sXBP1 mRNA levels in lung tissues wildtype (WT) and Prx2$^{-/-}$ mice under normoxia (N) *p < 0.05 compared to wildtype. Each sample is a pool from 5 mice. Representative of three independent experiments **(A)**. ATF6, CHOP, GADD34, sXBP1 mRNA levels in lung tissues (normalized to GADPH) wildtype (WT) and Prx2$^{-/-}$ mice exposed to hypoxia for 10 h (10 h), 3 days (3D), 7 days (7D). Each sample is a pool from 5 mice. **(B)** ATF6 *p < 0.05 for WT mice 10 h vs 3D; 10 h vs 7D. ATF6 *p < 0.05 for Prx2$^{-/-}$ mice 10 h vs 3D; ^ p < 0.05 for WT mice 7D vs Prx2$^{-/-}$ mice 7D. CHOP *p < 0.05 for WT mice 10 h vs 3D; 10 h vs 7D. CHOP *p < 0.05 for Prx2$^{-/-}$ mice 10 h vs 3D; 10 h vs 7D; ^ p < 0.05 for WT mice 10 h vs Prx2$^{-/-}$ mice 10 h. GADD34 *p < 0.05 for WT mice 10 h vs 3D; 10 h vs 7D. GADD34 *p < 0.05 for Prx2$^{-/-}$ mice 10 h vs 3D. sXbp1 *p < 0.05 for WT mice 10 h vs 3D; 10 h vs 7D. ^ p < 0.05 for WT mice 7D vs Prx2$^{-/-}$ mice 3D and 7D. sXbp1 *p < 0.05 for Prx2$^{-/-}$ mice 10 h vs 3D. ^ p < 0.05 for WT mice 7D vs Prx2$^{-/-}$ mice 7D. **C.** Average mitral valve deceleration time (left panel) and pulmonary acceleration time (PAT) to ejection time (ET) ratio (right panel); *p < 0.05 vehicle treated Prx2$^{-/-}$ mice *vs* PEP Prx2 treated Prx2$^{-/-}$ mice; by one-way ANOVA followed by Newman-Keuls Multiple Comparison test. The black dashed lines have been added to the graph to favor visual comparison between the white bars *vs* the black bars. Representative images of mitral inflow pattern recorded by Doppler echo imaging in Prx2$^{-/-}$ mice treated with PEP Prx2 are shown in Fig. 4SA. **D.** Immunoblot analysis with specific antibodies against atrial natriuretic peptide (ANP), vascular adhesion molecule -1 (VCAM-1), intracellular adhesion-molecule- 1 (ICAM-1) and superoxide dismutase-1 (SOD-1) of heart from Prx2$^{-/-}$ mice under normoxia (lane 1) and exposed to 7 days (7D) hypoxia treated with either vehicle or PEP Prx2. One representative gel from six with similar results is presented; GAPDH was used as protein loading control. **Right panel**. Relative quantification of immunoreactivity (DU: Density Units) of ANP, VCAM-1, ICAM-1, SOD1 of heart from Prx2$^{-/-}$ mice under normoxia and exposed to 7 days (7D) hypoxia treated with either vehicle or PEP Prx2. Data are presented as means ± SD (n = 6); ^p < 0.05 compared to Prx2$^{-/-}$ normoxic mice; ° p < 005 compared to vehicle treated mice.

bodies containing damaged proteins (Fig. 7A). It is of note that the procaspase/caspase 3 ratio was also increased in both mouse models exposed to hypoxia, but to higher extent in Prx2$^{-/-}$ mice compared to wildtype (Fig. 7A).

As a proof of concept that Prx2 is important in the crossroad between hypoxia induced oxidation and autophagy, we evaluated the effects of PEP Prx2 treatment on autophagy in mice exposed to 3 days hypoxia. As shown in Fig. 7A, PEP Prx2 administration rescued the hypoxia induced activation of autophagy. These data indicate that Prx2 acts as multimodal cytoprotective system and is important to prevent the development of PAH.

4. Discussion

Here, we firstly show the novel role of Prx2 as lung multimodal cytoprotector against hypoxia induced PAH. Our data also indicate that Prx2 is required in management of the physiologic oxidation in lung under room air condition. In fact, normoxic Prx2$^{-/-}$ mice show we lung chronic inflammatory vasculopathy and vascular dysfunction, associated with activation of extracellular matrix remodeling. This is in agreement with previous studies in mouse models genetically lacking other anti-oxidant systems such as SOD-1, which show increased susceptibility to both acute and chronic lung injury [53–55].

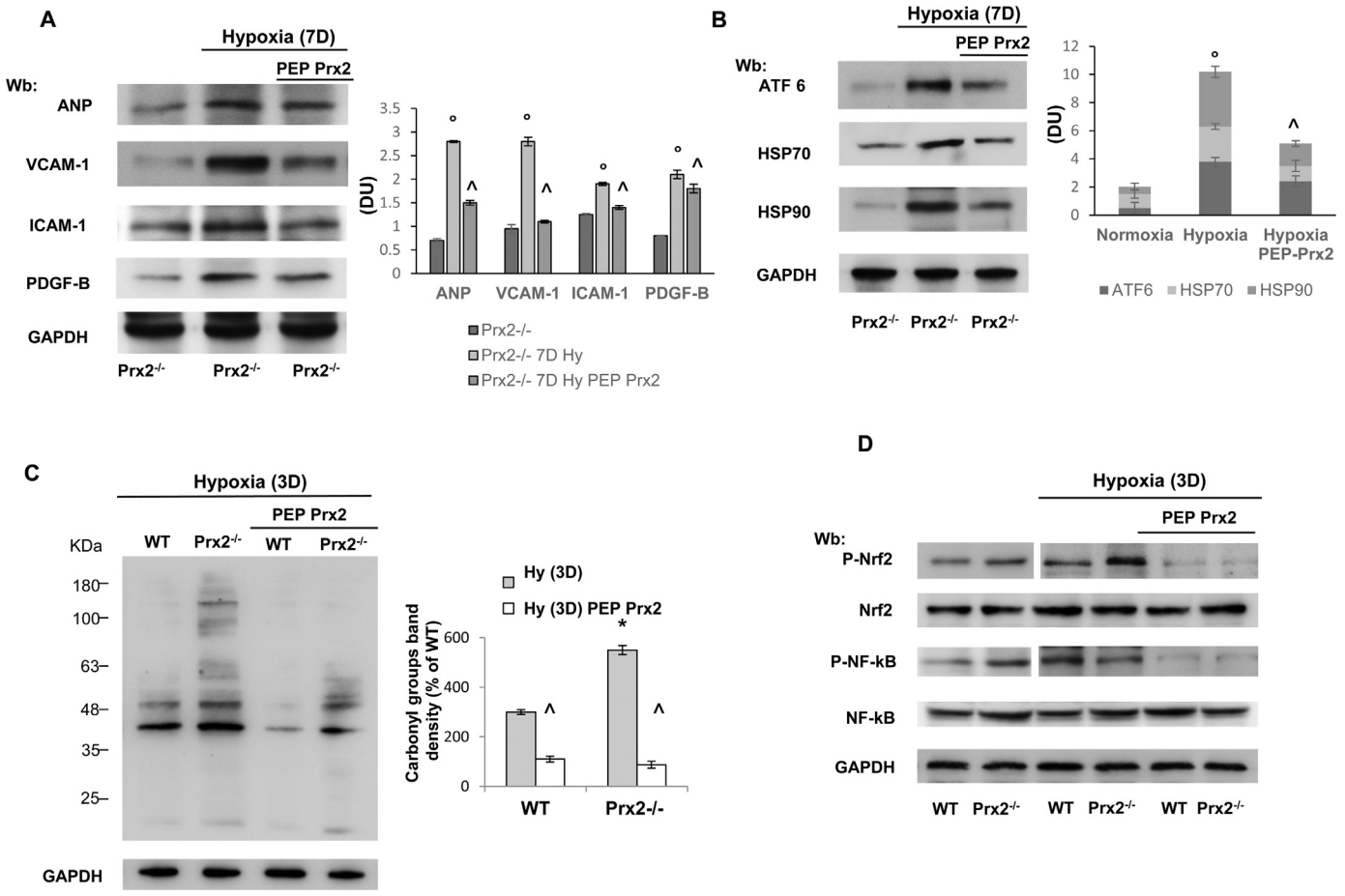

Fig. 5. PEP Prx2 administration prevents lung vascular remodeling and alleviates ER stress induced by prolonged hypoxia. A. Immunoblot analysis with specific antibodies against atrial natriuretic peptide (ANP), vascular adhesion molecule -1 (VCAM-1), intracellular adhesion-molecule- 1 (ICAM-1) and PDGF-B of lung from Prx2$^{-/-}$ mice under normoxia (lane 1) and exposed to 7 days (7D) hypoxia treated with either vehicle or PEP Prx2. One representative gel from six with similar results is presented; GAPDH was used as protein loading control. **Right panel.** Relative quantification of immunoreactivity (DU: Density Units) of ANP, VCAM-1, ICAM-1 and PDGF-B in lung from Prx2$^{-/-}$ mice under normoxia (lane 1) and exposed to 7 days (7D) hypoxia treated with either vehicle or PEP Prx2. Data are shown as means ± SD (n = 6); ^ $p < 0.05$ compared to Prx2$^{-/-}$ normoxic mice; ° $p < 0.05$ compared to Prx2$^{-/-}$ treated with vehicle. **B.** Immunoblot analysis with specific antibodies against activating transcriptional factor-6 (ATF6), heat shock protein 70 (HSP70) and heat shock protein 90 (HSP90) of lung from Prx2$^{-/-}$ mice under normoxia (lane 1) and exposed to 7 days (7D) hypoxia treated with either vehicle or PEP Prx2. One representative gel from six with similar results is presented; GAPDH was used as protein loading control. **Right panel.** Relative quantification of immunoreactivity (DU: Density Units) of ATF6, HSP70 and HSP90. Data are shown as means ± SD (n = 6); ^ $p < 0.05$ compared to Prx2$^{-/-}$ normoxic mice; ° $p < 0.05$ compared to Prx2$^{-/-}$ treated with vehicle. **C.** The carbonylated proteins (1 μg) were detected by treating with DNPH and blotted with anti-DNP antibody. **Right panel.** Quantification of band area was performed by densitometry and expressed as % of WT. The data are presented as means ± SD of at least three independent experiments *$p < 0.05$ compared to WT; ° $p < 0.05$ compared to vehicle treated mice (n = 3). **D.** Immunoblot analysis with specific antibodies against phospho-NF-kB (P-NF-kB), NF-kB, phospho-Nrf2 (P-Nrf2) and Nrf2 of lung from wildtype (WT) and Prx2$^{-/-}$ mice under normoxic condition treated with either vehicle or penetrating peptide fusion protein peroxiredoxin-2 (PEP Prx2). One representative gel from six with similar results is presented. Densitometric analysis of immunoblots is shown in Fig. 5SA.

Prx2$^{-/-}$ mice exposed to prolonged hypoxia developed signs of PAH, combined with inflammatory vasculopathy, sustained by high ET-1 expression and increased PDGF-B levels, as marker of extracellular matrix remodeling. Both molecules have been reported to accelerate the development of hypoxia induce PAH [30,39]. The increase ANP lung and heart expression indicates an attempt of endogenous system to induce pulmonary vaso-relaxation and to modulate lung and heart vascular remodeling in response to hypoxia [56,57]. This was coordinated by hypoxia induced activation of acute phase related transcriptional factors: Nrf2 and NF-kB in both mouse strains. The early and higher activation of Nrf2 in Prx2$^{-/-}$ mice compared to wildtype animals, supports the role of Nrf2 as back-up mechanism against severe oxidation in mice genetically lacking Prx2 [19]. Whereas, NF-kB seemed to be more important in prolonged hypoxia for wildtype mice compared to Prx2$^{-/-}$ animals. The rescue experiments with PEP Prx2 corroborate the importance of Prx2 in the functional cascade activated in response to hypoxia.

In this scenario, the absence of Prx2 favors ER stress with the activation of autophagy, as important mechanisms to deal with the accumulation of cytotoxic damaged proteins triggered by hypoxia and oxidation [10,44]. ER stress activates the UPR system, which is divided into three branches: ATF6, PERK and IRE1 [10,13]. In Prx2$^{-/-}$ mice, ATF6 was up-regulated in lung from animals under normoxia and after prolonged hypoxia. Whereas, GADD34, part of PERK branch, was early up-regulated at 3 days hypoxia in Prx2$^{-/-}$ mice. This indicate that the absence of Prx2 favors ER stress most likely due to a reduction of endogenous chaperone power beside the increased expression of classic heat shock proteins such as HSP70 and 90 in response to hypoxia. PEP Prx2 alleviated ER stress and prevented the hypoxia induced up-regulation of UPR system, in agreement with previous report on exogenous chemical chaperones, reducing ER stress and preventing the development of PAH [12,13]. It is of interest to note that previous reports have shown that PDGF-B and/or ET- activates UPR [13,43]. In our model, the absence of Prx2 resulted in high levels of PDGF-B and ET1 that potentiate the hypoxia induced activation of UPR system. The rescue experiments with PEP Prx2 corroborate the pivotal role of Prx2 in lung homeostasis.

The behavior of defensive autophagy in Prx2$^{-/-}$ mice exposed to

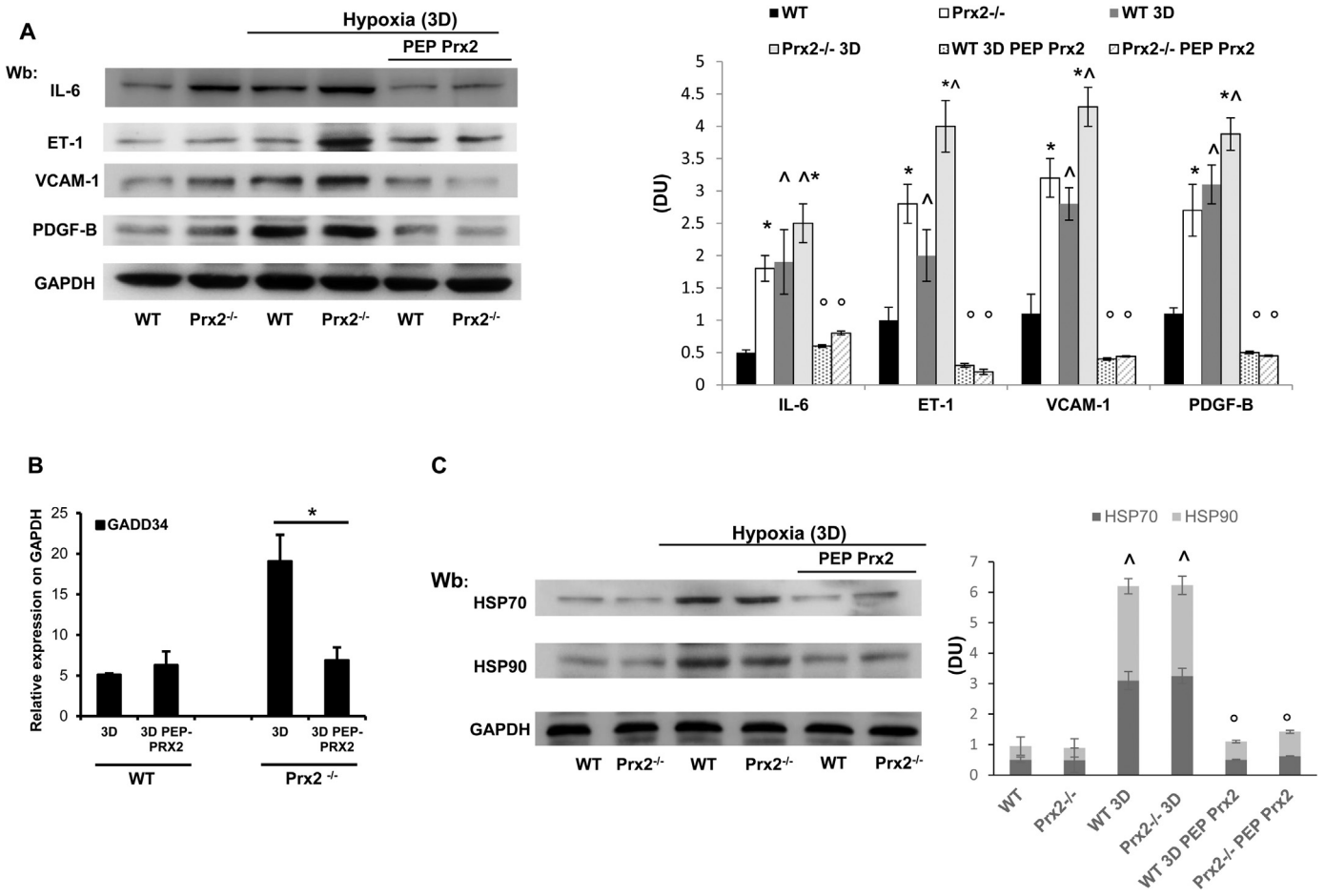

Fig. 6. PEP Prx2 administration reduces ER stress and prevents chaperone expression in the early phase of hypoxia. A. Immunoblot analysis with specific antibodies against IL-6, endothelin-1 (ET-1), vascular cell adhesion molecule-1 (VCAM-1), platelet derived growth factor-B (PDGF-B) of lung from wildtype (WT) and Prx2$^{-/-}$ mice under normoxic condition treated (lane 1–2) or exposed to hypoxia (3D) and treated with either vehicle or penetrating peptide fusion protein peroxiredoxin-2 (PEP Prx2). One representative gel from six with similar results is presented. GAPDH was used as loading control. **Right panel.** Relative quantification of immunoreactivity (DU: Density Units) of IL-6, ET-1, VCAM-1 and PDGF-B. Data are shown as means ± SD (n = 6). *p < 0.05 compared to wildtype; ^p < 0.05 compared to normoxic mice; °p < 005 compared to vehicle treated mice**. B.** GADD34 levels in lung tissues (normalized to GADPH) wildtype (WT) and Prx2$^{-/-}$ mice treated with either vehicle or penetrating peptide fusion protein peroxiredoxin-2 (PEP Prx2) exposed to hypoxia for 3D *p < 0.05 compared to wildtype. Each sample is a pool from 5 mice. Representative of three independent experiments. **C.** Immunoblot analysis with specific antibodies against heat shock protein-70 (HSP70) and -90 (HSP90) of lung from wildtype (WT) and Prx2$^{-/-}$ mice under normoxic condition treated (lane 1–2) or exposed to hypoxia (3D) and treated with either vehicle or penetrating peptide fusion protein peroxiredoxin-2 (PEP Prx2). One representative gel from six with similar results is presented. GAPDH was used as loading control. Right panel. **C.** Relative quantification of immunoreactivity (DU: Density Units) of HSP70 and HSP 90. Data are shown as means ± SD (n = 6); ^p < 0.05 compared to normoxic mice; °p < 005 compared to vehicle treated mice.

hypoxia is strongly linked to ER stress in the absence of Prx2. Treatment with PEP Prx2 reduced ER stress and switched-off autophagy as supported by the reduction in LC3II and accumulation of p62 (Fig. 6A). This was parallel by a decrease of hypoxia induced HSP70 and 90 expression and down-regulation of GADD34 and ATF6 levels in PEP Prx2 treated Prx2$^{-/-}$ mice exposed respectively to 3 and 7 days hypoxia.

Collectively, our data indicate that PEP Prx2 has a multimodal action targeting: (i) the inflammatory response; (ii) vascular and extracellular matrix remodeling, (iii) ER stress and autophagy (Fig. 7B). The correction of the imbalance between oxidation and anti-oxidant systems combined with a chaperone like function exerted by Prx2 might interrupt the vicious circle, established between oxidation-chronic inflammation with ER stress and activation of autophagy towards the generation of PAH (Fig. 7B).

In conclusion, we have firstly highlighted the novel pivotal role of Prx2 in preventing PAH induced by hypoxia. The high bio-complexity of PAH requires multimodal therapeutic approaches, which simultaneously act on different targets involved in its pathogenesis. Our data collectively support a rationale for considering Prx2 as novel therapeutic option in treatment of the early phase of PAH.

Authorship and contributions

EF, AM, LDF, IA, DM designed the experiments, analyzed data and wrote the paper; AJ, CL carried out the histologic analysis; AM, AS, LDF carried out the experiments; IA performed the molecular experiments and analyzed the data; CSY and KDW generated the PEP Prx2; SL carried out MDA measurements and analyzed data.

Conflict of interest and disclosure

The authors have nothing to disclose.

Acknowledgments

This work was supported by PRIN (LDF and AI: 201228PNX83) and FUR_UNIVR (LDF) 2016_2017.

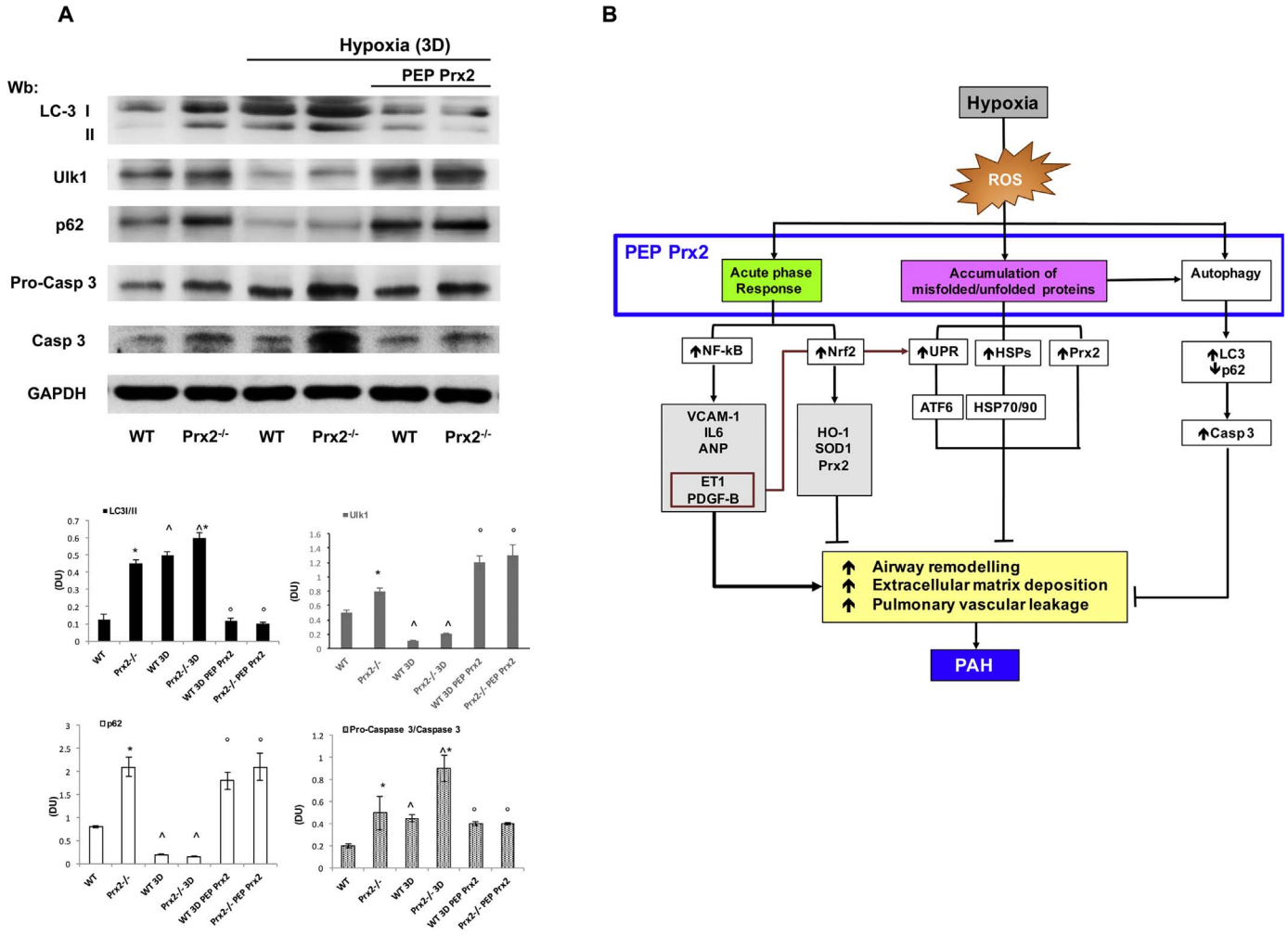

Fig. 7. A. Immunoblot analysis with specific antibodies against LC3I/II, Ulk1, p62, pro-caspase-caspase 3 of lung from wildtype (WT) and Prx2$^{-/-}$ mice under normoxic condition or exposed to 3 days (3D) hypoxia/reoxygenation stress (H/R) treated with either vehicle or penetrating peptide fusion protein peroxiredoxin-2 (PEP Prx2). One representative gel from six with similar results is presented. **Lower panel.** Relative quantification of immunoreactivity (DU: Density Units) of LC3I/II, Ulk1, p62, pro-caspase-caspase 3. Data are shown as means ± SD (n = 6). *p < 0.05 compared to wildtype; ° p < 0.05 compared to vehicle treated mice; ^ p < 0.05 compared to normoxic mice. **B.** Diagram of the novel role of Prx2 in pathogenesis of PAH induced by hypoxia and the novel multimodal action of Prx2 against hypoxia induce cytotoxic effects. Hypoxia promotes oxidation and induces acute phase inflammatory response, which is related to the activation of Nrf2, NF-kB. In the meantime, the accumulation of damage of cellular organelles and proteins results in activation of UPR system to limit endoplasmic reticulum (ER) stress, associated with increased expression of classical chaperones such as heat shock protein 70 and 90, and Prx2. ER stress leads to activation of autophagy as secondary mechanism to degraded damage proteins and reduce ER stress. This is supported by (i) conversion of LC3I to LC3II; and (ii) clearance of p62 positive lysosomes combined with the activation of caspase 3 pathway. PEP Prx2 treatment (i) prevents the hypoxia induced acute phase response activation of transcriptional factors NF-kB and Nrf2, (ii) alleviates ER stress related to hypoxia with reduction of ATF6 levels and (iii) blocks hypoxia induced autophagy. This results in reduction in markers of vascular remodeling, of extracellular matrix deposition and the abnormalities in pulmonary vascular leakage. ET1: endothelin 1; HO-1: heme-oxygenase-1; SOD1:superoxide dismutase; NF-kB: nuclear factor kappa-light-chain-enhancer of activated B cells; Nrf2: nuclear erythroid factor 2; P: phosphorylate form of indicated transcriptional factor; VCAM-1: vascular cell adhesion molecule -1; IL6:interleukin 6; PDGF-B: platelet derived growth factor-B; Casp 3: caspase 3; ANP: atrial natriuretic peptide; PEP Prx2: recombinant fusion penetrating protein Prx2; Prx2: peroxiredoxin-2; UPR: unfolded protein response; ATF6: activating transcriptional factor 6, HSPs: heat shock proteins, HSP70: heat shock protein-70, HSP90: heat shock protein-90; VCAM-1: vascular cell adhesion molecule 1; LC3 I/II: microtubule-associated protein 1A/1B-light chain 3.

Appendix A. Supporting information

Supplementary data associated with this article can be found in the online version at http://dx.doi.org/10.1016/j.freeradbiomed.2017.08.004.

References

[1] D.K. Rawat, A. Alzoubi, R. Gupte, S. Chettimada, M. Watanabe, A.G. Kahn, T. Okada, I.F. McMurtry, S.A. Gupte, Increased reactive oxygen species, metabolic maladaptation, and autophagy contribute to pulmonary arterial hypertension-induced ventricular hypertrophy and diastolic heart failure, Hypertension 64 (2014) 1266–1274.

[2] I.N. Zelko, R.J. Folz, Regulation of oxidative stress in pulmonary artery endothelium. modulation of extracellular superoxide dismutase and NOX4 expression using histone deacetylase class I inhibitors, Am. J. Respir. Cell Mol. Biol. 53 (2015) 513–524.

[3] S. Aggarwal, C.M. Gross, S. Sharma, J.R. Fineman, S.M. Black, Reactive oxygen species in pulmonary vascular remodeling, Compr. Physiol. 3 (2013) 1011–1034.

[4] D. Morales-Cano, C. Menendez, E. Moreno, J. Moral-Sanz, B. Barreira, P. Galindo, R. Pandolfi, R. Jimenez, L. Moreno, A. Cogolludo, J. Duarte, F. Perez-Vizcaino, The flavonoid quercetin reverses pulmonary hypertension in rats, PLoS One 9 (2014) e114492.

[5] B. Van Houten, Pulmonary arterial hypertension is associated with oxidative stress-induced genome instability, Am. J. Respir. Crit. Care Med. 192 (2015) 129–130.

[6] M.C. Chaumais, B. Ranchoux, D. Montani, P. Dorfmuller, L. Tu, F. Lecerf, N. Raymond, C. Guignabert, L. Price, G. Simonneau, S. Cohen-Kaminsky, M. Humbert, F. Perros, N-acetylcysteine improves established monocrotaline-induced pulmonary hypertension in rats, Respir. Res. 15 (2014) 65.

[7] H.H. Schmidt, R. Stocker, C. Vollbracht, G. Paulsen, D. Riley, A. Daiber, A. Cuadrado, Antioxidants in translational medicine, Antioxid. Redox Signal. 23 (2015) 1130–1143.

[8] R. Scherz-Shouval, Z. Elazar, Regulation of autophagy by ROS: physiology and pathology, Trends Biochem. Sci. 36 (2011) 30–38.

[9] S. Kongara, V. Karantza, The interplay between autophagy and ROS in tumorigenesis, Front. Oncol. 2 (2012) 171.

[10] R. Sano, J.C. Reed, ER stress-induced cell death mechanisms, Biochim. Biophys. Acta 1833 (2013) 3460–3470.

[11] G. Wang, S. Liu, L. Wang, L. Meng, C. Cui, H. Zhang, S. Hu, N. Ma, Y. Wei, Lipocalin-2 promotes endoplasmic reticulum stress and proliferation by augmenting intracellular iron in human pulmonary arterial smooth muscle cells, Int. J. Biol. Sci. 13 (2017) 135–144.

[12] P. Dromparis, R. Paulin, T.H. Stenson, A. Haromy, G. Sutendra, E.D. Michelakis, Attenuating endoplasmic reticulum stress as a novel therapeutic strategy in pulmonary hypertension, Circulation 127 (2013) 115–125.

[13] M. Koyama, M. Furuhashi, S. Ishimura, T. Mita, T. Fuseya, Y. Okazaki, H. Yoshida, K. Tsuchihashi, T. Miura, Reduction of endoplasmic reticulum stress by 4-phenylbutyric acid prevents the development of hypoxia-induced pulmonary arterial hypertension, Am. J. Physiol. Heart Circ. Physiol. 306 (2014) H1314–H1323.

[14] G.K. Wang, S.H. Li, Z.M. Zhao, S.X. Liu, G.X. Zhang, F. Yang, Y. Wang, F. Wu, X.X. Zhao, Z.Y. Xu, Inhibition of heat shock protein 90 improves pulmonary arteriole remodeling in pulmonary arterial hypertension, Oncotarget 7 (2016) 54263–54273.

[15] F.M. Low, M.B. Hampton, A.V. Peskin, C.C. Winterbourn, Peroxiredoxin 2 functions as a noncatalytic scavenger of low-level hydrogen peroxide in the erythrocyte, Blood 109 (2007) 2611–2617.

[16] S.G. Rhee, H.A. Woo, Multiple functions of peroxiredoxins: peroxidases, sensors and regulators of the intracellular messenger H(2)O(2), and protein chaperones, Antioxid. Redox Signal. 15 (2011) 781–794.

[17] A. Matte, A. Pantaleo, E. Ferru, F. Turrini, M. Bertoldi, F. Lupo, A. Siciliano, C. Ho Zoon, L. De Franceschi, The novel role of peroxiredoxin-2 in red cell membrane protein homeostasis and senescence, Free Radic. Biol. Med. 76C (2014) 80–88.

[18] F.M. Low, M.B. Hampton, C.C. Winterbourn, Peroxiredoxin 2 and peroxide metabolism in the erythrocyte, Antioxid. Redox Signal. 10 (2008) 1621–1630.

[19] A. Matte, L. De Falco, A. Iolascon, N. Mohandas, X. An, A. Siciliano, C. Leboeuf, A. Janin, M. Bruno, S.Y. Choi, D.W. Kim, L. De Franceschi, The interplay between peroxiredoxin-2 and nuclear factor-erythroid 2 is important in limiting oxidative mediated dysfunction in beta-thalassemic erythropoiesis, Antioxid. Redox Signal. 23 (2015) 1284–1297.

[20] S.S. Franco, L. De Falco, S. Ghaffari, C. Brugnara, D.A. Sinclair, A. Matte, A. Iolascon, N. Mohandas, M. Bertoldi, X. An, A. Siciliano, P. Rimmele, M.D. Cappellini, S. Michan, E. Zoratti, J. Anne, L. De Franceschi, Resveratrol accelerates erythroid maturation by activation of FoxO3 and ameliorates anemia in beta-thalassemic mice, Haematologica 99 (2014) 267–275.

[21] A. Matte, P.S. Low, F. Turrini, M. Bertoldi, M.E. Campanella, D. Spano, A. Pantaleo, A. Siciliano, L. De Franceschi, Peroxiredoxin-2 expression is increased in beta-thalassemic mouse red cells but is displaced from the membrane as a marker of oxidative stress, Free Radic. Biol. Med. 49 (2010) 457–466.

[22] D. Yang, Y. Song, X. Wang, J. Sun, Y. Ben, X. An, L. Tong, J. Bi, X. Wang, C. Bai, Deletion of peroxiredoxin 6 potentiates lipopolysaccharide-induced acute lung injury in mice, Crit. Care Med. 39 (2011) 756–764.

[23] C.S. Yang, D.S. Lee, C.H. Song, S.J. An, S. Li, J.M. Kim, C.S. Kim, D.G. Yoo, B.H. Jeon, H.Y. Yang, T.H. Lee, Z.W. Lee, J. El-Benna, D.Y. Yu, E.K. Jo, Roles of peroxiredoxin II in the regulation of proinflammatory responses to LPS and protection against endotoxin-induced lethal shock, J. Exp. Med. 204 (2007) 583–594.

[24] Y. Gan, X. Ji, X. Hu, Y. Luo, L. Zhang, P. Li, X. Liu, F. Yan, P. Vosler, Y. Gao, R.A. Stetler, J. Chen, Transgenic overexpression of peroxiredoxin-2 attenuates ischemic neuronal injury via suppression of a redox-sensitive pro-death signaling pathway, Antioxid. Redox Signal. 17 (2012) 719–732.

[25] S. Boulos, B.P. Meloni, P.G. Arthur, C. Bojarski, N.W. Knuckey, Peroxiredoxin 2 overexpression protects cortical neuronal cultures from ischemic and oxidative injury but not glutamate excitotoxicity, whereas Cu/Zn superoxide dismutase 1 overexpression protects only against oxidative injury, J. Neurosci. Res. 85 (2007) 3089–3097.

[26] L. de Franceschi, F. Turrini, M. Honczarenko, K. Ayi, A. Rivera, M.D. Fleming, T. Law, F. Mannu, F.A. Kuypers, A. Bast, W.J. van der Vijgh, C. Brugnara, In vivo reduction of erythrocyte oxidant stress in a murine model of beta-thalassemia, Haematologica 89 (2004) 1287–1298.

[27] B.T. Kalish, A. Matte, I. Andolfo, A. Iolascon, O. Weinberg, A. Ghigo, J. Cimino, A. Siciliano, E. Hirsch, E. Federti, M. Puder, C. Brugnara, L. De Franceschi, Dietary omega-3 fatty acids protect against vasculopathy in a transgenic mouse model of sickle cell disease, Haematologica 100 (2015) 870–880.

[28] L. De Franceschi, C. Brugnara, P. Rouyer-Fessard, H. Jouault, Y. Beuzard, Formation of dense erythrocytes in SAD mice exposed to chronic hypoxia: evaluation of different therapeutic regimens and of a combination of oral clotrimazole and magnesium therapies, Blood 94 (1999) 4307–4313.

[29] L. Dalle Carbonare, A. Matte, M.T. Valenti, A. Siciliano, A. Mori, V. Schweiger, G. Zampieri, L. Perbellini, L. De Franceschi, Hypoxia-reperfusion affects osteogenic lineage and promotes sickle cell bone disease, Blood 126 (2015) 2320–2328.

[30] N. Sabaa, L. de Franceschi, P. Bonnin, Y. Castier, G. Malpeli, H. Debbabi, A. Galaup, M. Maier-Redelsperger, S. Vandermeersch, A. Scarpa, A. Janin, B. Levy, R. Girot, Y. Beuzard, C. Leboeuf, A. Henri, S. Germain, J.C. Dussaule, P.L. Tharaux, Endothelin receptor antagonism prevents hypoxia-induced mortality and morbidity in a mouse model of sickle-cell disease, J. Clin. Investig. 118 (2008) 1924–1933.

[31] A. Matte, M. Bertoldi, N. Mohandas, X. An, A. Bugatti, A.M. Brunati, M. Rusnati, E. Tibaldi, A. Siciliano, F. Turrini, S. Perrotta, L. De Franceschi, Membrane association of peroxiredoxin-2 in red cells is mediated by the N-terminal cytoplasmic domain of band 3, Free Radic. Biol. Med. 55 (2013) 27–35.

[32] R. Bellelli, G. Federico, A. Matte, D. Colecchia, A. Iolascon, M. Chiariello, M. Santoro, L. De Franceschi, F. Carlomagno, NCOA4 deficiency impairs systemic iron homeostasis, Cell Rep. 14 (2016) 411–421.

[33] L. De Franceschi, F. Turrini, E.M. del Giudice, S. Perrotta, O. Olivieri, R. Corrocher, F. Mannu, A. Iolascon, Decreased band 3 anion transport activity and band 3 clusterization in congenital dyserythropoietic anemia type II, Exp. Hematol. 26 (1998) 869–873.

[34] V. Kumar, N. Kitaeff, M.B. Hampton, M.B. Cannell, C.C. Winterbourn, Reversible oxidation of mitochondrial peroxiredoxin 3 in mouse heart subjected to ischemia and reperfusion, FEBS Lett. 583 (2009) 997–1000.

[35] A. Cozzi, B. Corsi, S. Levi, P. Santambrogio, A. Albertini, P. Arosio, Overexpression of wild type and mutated human ferritin H-chain in HeLa cells: in vivo role of ferritin ferroxidase activity, J. Biol. Chem. 275 (2000) 25122–25129.

[36] L. De Franceschi, O.S. Platt, G. Malpeli, A. Janin, A. Scarpa, C. Leboeuf, Y. Beuzard, E. Payen, C. Brugnara, Protective effects of phosphodiesterase-4 (PDE-4) inhibition in the early phase of pulmonary arterial hypertension in transgenic sickle cell mice, FASEB J. 22 (2008) 1849–1860.

[37] G. Ingoglia, C.M. Sag, N. Rex, L. De Franceschi, F. Vinchi, J. Cimino, S. Petrillo, S. Wagner, K. Kreitmeier, L. Silengo, F. Altruda, L.S. Maier, E. Hirsch, A. Ghigo, E. Tolosano, Hemopexin counteracts systolic dysfunction induced by heme-driven oxidative stress, Free Radic. Biol. Med. 108 (2017) 452–464.

[38] S.K. Niture, R. Khatri, A.K. Jaiswal, Regulation of Nrf2-an update, Free Radic. Biol. Med. 66 (2014) 36–44.

[39] R.T. Schermuly, E. Dony, H.A. Ghofrani, S. Pullamsetti, R. Savai, M. Roth, A. Sydykov, Y.J. Lai, N. Weissmann, W. Seeger, F. Grimminger, Reversal of experimental pulmonary hypertension by PDGF inhibition, J. Clin. Investig. 115 (2005) 2811–2821.

[40] M. Thamsen, C. Kumsta, F. Li, U. Jakob, Is overoxidation of peroxiredoxin physiologically significant? Antioxid. Redox Signal. 14 (2011) 725–730.

[41] A. Adegunsoye, J. Balachandran, Inflammatory response mechanisms exacerbating hypoxemia in coexistent pulmonary fibrosis and sleep apnea, Mediat. Inflamm. 2015 (2015) 510105.

[42] M. Fartoukh, D. Emilie, C. Le Gall, G. Monti, G. Simonneau, M. Humbert, Chemokine macrophage inflammatory protein-1alpha mRNA expression in lung biopsy specimens of primary pulmonary hypertension, Chest 114 (1998) 50S–51S.

[43] M.E. Yeager, D.D. Belchenko, C.M. Nguyen, K.L. Colvin, D.D. Ivy, K.R. Stenmark, Endothelin-1, the unfolded protein response, and persistent inflammation: role of pulmonary artery smooth muscle cells, Am. J. Respir. Cell Mol. Biol. 46 (2012) 14–22.

[44] S. Bernales, K.L. McDonald, P. Walter, Autophagy counterbalances endoplasmic reticulum expansion during the unfolded protein response, PLoS Biol. 4 (2006) e423.

[45] G. Sutendra, P. Dromparis, P. Wright, S. Bonnet, A. Haromy, Z. Hao, M.S. McMurtry, M. Michalak, J.E. Vance, W.C. Sessa, E.D. Michelakis, The role of Nogo and the mitochondria-endoplasmic reticulum unit in pulmonary hypertension, Sci. Transl. Med. 3 (2011) 88ra55.

[46] J.C. Moon, Y.S. Hah, W.Y. Kim, B.G. Jung, H.H. Jang, J.R. Lee, S.Y. Kim, Y.M. Lee, M.G. Jeon, C.W. Kim, M.J. Cho, S.Y. Lee, Oxidative stress-dependent structural and functional switching of a human 2-Cys peroxiredoxin isotype II that enhances HeLa cell resistance to H2O2-induced cell death, J. Biol. Chem. 280 (2005) 28775–28784.

[47] A.V. Peskin, N. Dickerhof, R.A. Poynton, L.N. Paton, P.E. Pace, M.B. Hampton, C.C. Winterbourn, Hyperoxidation of peroxiredoxins 2 and 3: rate constants for the reactions of the sulfenic acid of the peroxidatic cysteine, J. Biol. Chem. 288 (2013) 14170–14177.

[48] Q. Li, Y. Qiu, M. Mao, J. Lv, L. Zhang, S. Li, X. Li, X. Zheng, Antioxidant mechanism of Rutin on hypoxia-induced pulmonary arterial cell proliferation, Molecules 19 (2014) 19036–19049.

[49] M.C. Sobotta, A.G. Barata, U. Schmidt, S. Mueller, G. Millonig, T.P. Dick, Exposing cells to H2O2: a quantitative comparison between continuous low-dose and one-time high-dose treatments, Free Radic. Biol. Med. 60 (2013) 325–335.

[50] G. Marino, M. Niso-Santano, E.H. Baehrecke, G. Kroemer, Self-consumption: the interplay of autophagy and apoptosis, Nat. Rev. Mol. Cell Biol. 15 (2014) 81–94.

[51] J. Xiong, Atg7 in development and disease: panacea or Pandora's Box? Protein Cell 6 (2015) 722–734.

[52] F. Lupo, E. Tibaldi, A. Matte, A.K. Sharma, A.M. Brunati, S.L. Alper, C. Zancanaro, D. Benati, A. Siciliano, M. Bertoldi, F. Zonta, A. Storch, R.H. Walker, A. Danek, B. Bader, A. Hermann, L. De Franceschi, A new molecular link between defective autophagy and erythroid abnormalities in chorea-acanthocytosis, Blood 128 (2016) 2976–2987.

[53] C. Delaney, R.H. Wright, J.R. Tang, C. Woods, L. Villegas, L. Sherlock, R.C. Savani, S.H. Abman, E. Nozik-Grayck, Lack of EC-SOD worsens alveolar and vascular development in a neonatal mouse model of bleomycin-induced bronchopulmonary dysplasia and pulmonary hypertension, Pediatr. Res. 78 (2015) 634–640.

[54] T. Zhuang, M. Zhang, H. Zhang, P.A. Dennery, Q.S. Lin, Disrupted postnatal lung development in heme oxygenase-1 deficient mice, Respir. Res. 11 (2010) 142.

[55] O.D. Liang, S.A. Mitsialis, M.S. Chang, E. Vergadi, C. Lee, M. Aslam, A. Fernandez-Gonzalez, X. Liu, R. Baveja, S. Kourembanas, Mesenchymal stromal cells expressing heme oxygenase-1 reverse pulmonary hypertension, Stem Cells 29 (2011) 99–107.

[56] D. Wang, I.P. Gladysheva, T.H. Fan, R. Sullivan, A.K. Houng, G.L. Reed, Atrial natriuretic peptide affects cardiac remodeling, function, heart failure, and survival in a mouse model of dilated cardiomyopathy, Hypertension 63 (2014) 514–519.

[57] F. Werner, B. Kojonazarov, B. Gassner, M. Abesser, K. Schuh, K. Volker, H.A. Baba, B.K. Dahal, R.T. Schermuly, M. Kuhn, Endothelial actions of atrial natriuretic peptide prevent pulmonary hypertension in mice, Basic Res. Cardiol. 111 (2016) 22.